

An Experimental and Theoretical Study of Jet-Cooled Complexes of Chiral Molecules: The Role of Dispersive Forces in Chiral Discrimination

K. Le Barbu,[†] V. Brenner,[‡] Ph. Millié,[‡] F. Lahmani,[†] and A. Zehnacker-Rentien^{*,†}

Laboratoire de Photophysique Moléculaire du CNRS, Bât. 210 Université de Paris XI, F-91405 Orsay Cedex, France, and DRECAM-SPAM, CEN Saclay, F-91191 Gif sur Yvette, France

Received: July 28, 1997; In Final Form: October 13, 1997[⊗]

Isomer formation in dimeric complexes of a chiral naphthalene derivative (2-naphthyl-1-ethanol) with nonchiral or chiral primary and secondary alcohols (*n*-propanol, 2-methyl-1-butanol, 2-butanol, 2-pentanol) has been studied by hole-burning spectroscopy. Besides the spectroscopic discrimination between the homochiral and heterochiral complexes, previously observed in the fluorescence excitation spectra, ground-state depletion experiments have shown that each diastereoisomer is cooled in the jet in several isomeric forms. To get information on the structures of the complexes and on the influence of the solvent conformations of these structures, semiempirical calculations that rely on the exchange perturbation method have been performed. It has been shown that the most stable complexes involve a H-bond between the chromophore acting as the donor and the solvent and that they involve anti and gauche conformations of the solvent. The binding energy of the complexes results from a subtle balance between electrostatic and dispersive forces: the complexes involving the gauche and anti conformers of the solvent differ from each other by the amount of dispersion energy relative to the total interaction energy. The increase in the dispersive forces calculated for the complexes with the anti conformers has been related to a larger red shift of the absorption spectrum and is suggested to play a role in the observed chiral discrimination.

Introduction

Chiral discrimination is of the widest importance in life-chemistry and takes place through stereoselective interactions with an optically active selecting agent in a diastereoisomeric contact pair implying short-range forces.^{1,2} Modern chemical methods which allow the separation of enantiomers, such as chiral phase-chromatography, rely also on a very small difference between the interaction energy of a chiral molecule with a chiral surrounding, depending on the enantiomer.^{3,4} Since the weak molecular interactions at play in chiral discrimination imply mostly transient complexes and are difficult to investigate in solution at room temperature, we have recently undertaken a spectroscopic study of van der Waals complexes of chiral molecules bearing an asymmetric carbon by means of the supersonic jet technique combined with laser-induced fluorescence.^{5–7} By stabilizing weakly bound diastereoisomers isolated in the gas phase, this technique provides a powerful tool for studying the short-range molecular interactions involved in chiral recognition from a microscopic point of view. We have recently reported on the spectroscopy of van der Waals complexes of a chiral chromophore 2-naphthyl-1-ethanol, denoted NapEtOH hereafter, complexed by a series of either nonchiral or chiral aliphatic alcohols.⁶ For each chiral alcohol studied, chiral discrimination has been unambiguously evidenced on the basis of a different spectral shift of the S_0-S_1 transition. However, the fluorescence excitation spectrum was complicated by the presence of numerous features that suggest the formation

of several isomers. This is the reason why we have extended our previous conventional fluorescence measurements to ground-state depletion (hole-burning) experiments. This technique allows discrimination between different ground-state isomers^{8–13} and the recording of the absorption spectrum of species that absorb in the same energy range. It has been applied to numerous systems, either bare molecules such as phenethylamine,¹³ complexes between aromatic species and rare gas or alkane molecules,¹¹ hydrogen-bonded systems such as 9-methoxyanthracene:methanol,^{9–12} or donor–acceptor complexes such as anthracene–dialkylaniline.^{10–12} We have applied this technique to the complexes of NapEtOH with chiral (2-butanol, 2-pentanol, 1-methyl-2-butanol) alcohols and a model alcohol 1-propanol. In order to obtain a better understanding at the microscopic level of the nature of the contact pair, we have compared the experimental results with theoretical calculations based on the exchange–perturbation method.¹⁴

The first question we want to address concerns the nature of the forces responsible for chiral discrimination: it is often proposed^{3–4,15–17} that chiral recognition is achieved if the chiral centers interact via a minimum of three simultaneous interactions, with at least one of these interactions being stereochemically dependent. These interactions may be either localized (for example hydrogen bonding) or nonlocal in nature, as in a dispersive interaction. Several authors mention multiple H-bonds as a means to facilitate chiral recognition such as in the diol–diamine systems.^{15,16} Moreover, it is often observed that an aromatic substituent in a chiral selecting agent increases its efficiency by offering supplementary interactions to the chiral partner.¹⁷ In the present study, the chromophore and the solvents both display a OH group, and one expects the

[†] Université de Paris XI.

[‡] DRECAM-SPAM.

[⊗] Abstract published in *Advance ACS Abstracts*, December 1, 1997.

complexes to be bound by a H-bond, which is known to be a strong and directional interaction. As the chromophore under study also involves a naphthalene subunit, additional forces involving the aromatic ring (dispersion forces) may play a role in the stabilization of the complex. This system will thus provide information on the role of the different forces at play (H-bond vs dispersion–repulsion) in chiral recognition.

Another important question is the role of the conformational isomerism in chiral discrimination: If the chiral molecules to be discriminated are flexible and exist as different rotational isomers, a given conformation of a chiral molecule may present more easily than others the geometry that allows stereospecific interaction with the selecting agent. This has been discussed, for example, in the case of chiral phase chromatography,³ in which a three point interaction may be obtained only for a specific conformation of the solute. In the system studied here, both experimental and theoretical results show that the chromophore exists under a single conformation.⁶ The alcohols used here as a solvent are floppy: several ground-state conformers may coexist in the supersonic jet and are expected to be discriminated in a different way by the chiral chromophore. Conformational isomerism can thus provide a very sensitive probe of the weak molecular forces implied in chiral recognition.

Experimental Section

The experiment is based on the laser excitation of van der Waals complexes formed in a continuous supersonic expansion of helium (2–3 atm) and has been reported previously.¹⁸ The molecules are excited in the cold region of the jet by means of a frequency-doubled dye laser (Rh640 and DCM) pumped by the second harmonic of a YAG laser (BM Industrie or Quantel). The fluorescence is observed at right angles through a WG335 cutoff filter by a Hamamatsu R2059 photomultiplier. The signal is monitored by a Camac ADC (Lecroy 2249W) connected to a PC computer.

Hole-burning experiments in a supersonic jet were first reported by Lipert and Colson⁸ and involved a pump–probe excitation scheme: an intense laser beam scans through the wavelength region of interest (the pump) while a counterpropagating laser (the probe), delayed in time, is fixed on a selected resonance whose resulting fluorescence gives a measure of the population of the probed ground-state level. When both lasers excite transitions which arise from the same ground-state species, the pump beam induced depopulation manifests itself by a decrease in the intensity of the fluorescence excited by the probe (spectral hole). If both lasers excite different ground-state levels, no spectral hole is observed. Because of the long lifetime of the excited species, the delay between pump and probe is around 700 ns, and the pump and probe beams have to be separated in the jet by about 1 mm to take account of the speed of the species in the helium expansion.

Theoretical Methods

1. Molecular Interactions. The size of the systems under study precludes any meaningful *ab initio* calculation for the following reasons: Firstly, the dispersive forces play a significant role in the total interaction energy of such systems and a quantitative description of these forces requires a highly sophisticated atomic orbital basis set and post-SCF calculations. Such calculations are not tractable for large systems. Secondly, the basis set superposition error (BSSE) correction, which is nonnegligible for such systems, is evaluated at the end of the calculation for the optimized geometry; thus its dependence upon the complex geometry is not taken into account. Finally, since

an exploration of large portions of the potential energy surface must be performed in order to obtain the whole set of significant minima, local optimization methods are inefficient and nonlocal methods such as the simulated annealing method which requires a direct and rapid calculation of the intermolecular potential have to be used. Thus, the method developed by Claverie¹⁹ has been used to calculate the interaction energy. This method is a second-order perturbation treatment based on the “exchange perturbation” theory which consists of introducing the Pauli principle in the unperturbed wave function in order to take the “intersystem” exchanges into account. This method has already been applied to complexes composed of 1-cyanonaphthalene with acetonitrile and water¹⁴ and to anthracene–dialkylaniline systems.²⁰ The details of the method have already been described.^{21,22} For each order of perturbation, the intermolecular energy is written as the sum of the Rayleigh–Schrödinger term E_{rs} and an exchange term E_{ex} due to the antisymmetrization of the wave function relative to the intersystem exchange. Thus the intermolecular energy can be decomposed as the following:

$$E = E_{rs}^1 + E_{rs}^2 + E_{ex}^1 + E_{ex}^2$$

where E_{rs}^1 is the electrostatic term, E_{rs}^2 is the polarization and dispersion term, E_{ex}^1 is the exchange repulsion term, and E_{ex}^2 is the dispersion exchange term. All these terms can be written analytically as a function of the intermolecular distances. The electrostatic term is calculated as a sum of multipole–multipole interactions, and the polarization term is the sum of each molecular polarization energy due the electric field created by the multipoles of all the other molecules. The set of multipoles (a monopole, a dipole, and a quadrupole on each atom and one point per chemical bond) of each molecule is obtained by the procedure developed by Vigne-Maeder et al.²⁹ From the exact multipolar multicentric development of the electron distribution derived from the *ab initio* wave function, a simplified representation of the multipole distribution is generated through a systematic procedure of the reduction of the number of the centers (atoms plus barycenter of the bonds).³⁰ A detailed study of the effects of the basis set and intramolecular correlation on the interaction energy and its minima has shown that the multipole distribution of molecule must be derived from a correlated wave function within at least a double ζ plus polarization basis set.^{21,22} The polarizability of the centers are evaluated according to the number of electrons of atoms involved in the bonds and in lone pairs from mean bond polarizabilities which are obtained from the experimental longitudinal and transverse bond polarizabilities. The repulsion, dispersion, and dispersion–exchange terms are evaluated as a sum of atom–atom contributions. The repulsion term has been calculated by taking into account the influence of the electronic population variation on the van der Waals radius of each atom.^{21,22}

As the chromophore is a large molecule, its geometry has been optimized with the semiempirical AM1 method.²⁴ The alcohol molecules used as solvents present different conformations of very similar energy, and a more refined method of calculation is needed. Thus, the geometry optimization of the solvents have been performed at the MP2/6-31G** level by means of the Gaussian program.²⁵ For the optimized geometry of each molecule (chromophore and solvents), an *ab initio* calculation has been performed at the MP2/6-31G** level by means of the Gaussian program to obtain the wave function. The 6-31G basis set used here²³ includes one set of polarization functions for C(0.63), O(1.33), and H(0.8).

Furthermore, a charge distribution for each conformer has been calculated separately since it is often admitted that the distribution of conformers in the gas mixture before the expansion²⁶ is preserved after cooling, provided the barrier between them is higher than 1.4 kcal/mol. Here, the barrier between different conformers of the solvent is estimated around 3 kcal/mol.^{27,28}

2. Potential Energy Surfaces (PESs). The minima localization procedure used is an extension of the simulated annealing method, similar to the procedure used by Liotard.³⁰ Efficient determination of minima on the potential energy surface is ensured by a combination of global (simulated annealing)^{31a} and local (quasi-Newton)^{31b} methods. In the determination of the minima, a modified simulated annealing algorithm is used to locate the portions corresponding to the attractive areas on the PESs and one configuration of each significant portion is optimized by a local method. True minima are then characterized by a scrutiny of the Hessian eigenvalues.

For the saddle point localization, we have used the method of the chain developed by Liotard.³² It consists of the energetic relaxation on the potential energy surface of a path connecting the two minima. This relaxation is performed until the highest point of the path cannot be relaxed any further, i.e., until the gradient at the highest energy point is nearly parallel to the path. It is important to notice that this method is local in nature since it depends on the starting saddle point.

Results

1. Excitation and Hole-Burning Spectroscopy. The laser-induced fluorescence spectrum of the racemic NapEtOH compound (which is strictly identical to that of *R*-NapEtOH or *S*-NapEtOH) has been previously reported.⁵ Its 0_0^0 transition located at 31738.4 cm^{-1} is followed by two low-frequency features at 39 and 76 cm^{-1} assigned to a torsion motion of the $\text{CH}(\text{CH}_3)\text{OH}$ group by analogy with 2-ethyl naphthalene³³ or benzyl alcohol³⁴ where similar low-frequency modes are observed. Hole-burning spectra obtained with the probe laser fixed on the most intense origin band shows that the three features of the bare molecule are due to the same isomer, as observed for benzyl alcohol.³⁴ This contrasts with other benzene derivatives, such as phenethylamine where the presence of several isomers has been deduced from hole-burning spectroscopy experiments.¹³

A. Primary Alcohols. a. NapEtOH/1-Propanol (1-PrOH) Complexes. The fluorescence excitation spectrum of the NapEtOH/1-PrOH complex, together with the hole-burning spectra in the region of the $S_0 \rightarrow S_1$ origin of the bare chromophore, is presented in Figure 1. The formation of the complex manifests itself by the appearance of four main features located at -138, -112, -60, and -55 cm^{-1} , respectively, from the 0_0^0 transition of NapEtOH. Hole-burning experiments have been performed with the probe laser tuned on the features at -138, -60, and -55 cm^{-1} from the origin. These hole-burning spectra show unambiguously the presence of three isomers denoted hereafter IP1, IP2, and IP3. The 0_0^0 transitions of IP1, IP2, and IP3 are located at -138, -60, and -55 cm^{-1} from that of NapEtOH, respectively. IP2 and IP3 display a single intense feature separated from each other by only 5 cm^{-1} and appear as a doublet in the fluorescence excitation spectrum, whereas the excitation spectrum of IP1 exhibits a larger red shift and two main bands located at -138 and -112 cm^{-1} that involve a low-frequency mode of 26 cm^{-1} .

b. NapEtOH/2-Methyl-1-Butanol (2-Me-1-BuOH) Complexes. The fluorescence excitation spectra of the NapEtOH/

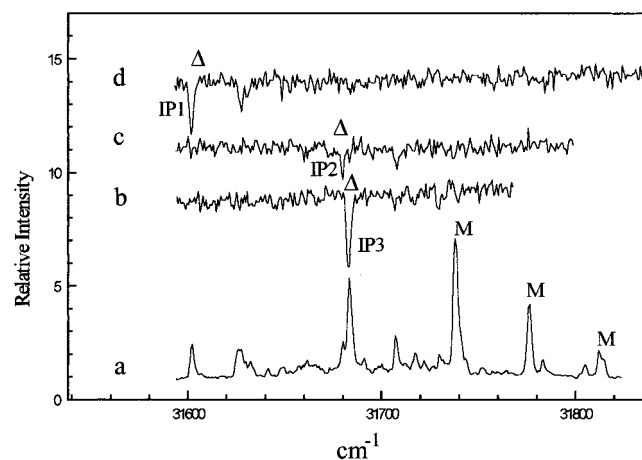


Figure 1. (a) Fluorescence excitation spectrum of the NapEtOH:1-propanol complex. Hole-burning spectrum obtained with the probe tuned on the transition denoted by Δ and located at (b) -55, (c) -60, (d) -138 cm^{-1} . The bands due to the bare chromophore are denoted by M.

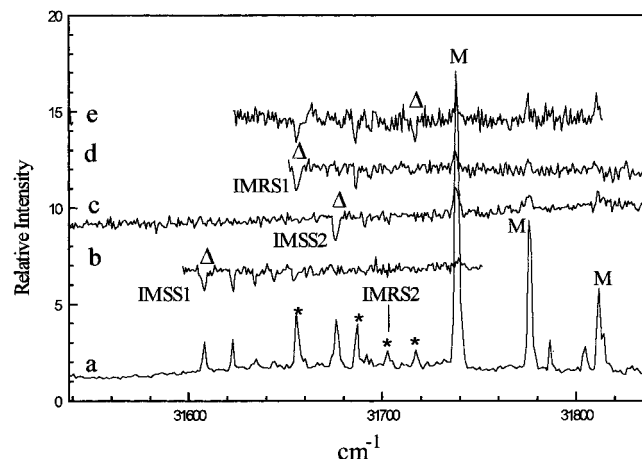


Figure 2. (a) Fluorescence excitation spectrum of the NapEtOH:1-methyl-2-butanol complex. Hole-burning spectrum obtained with the probe tuned on the transition denoted by Δ and located at (b) -134 cm^{-1} (*SS* complex), (c) -62 cm^{-1} (*SS* complex), (d) -84 cm^{-1} (*RS* complex), (e) -19 cm^{-1} (*RS* complex). The bands due to the bare chromophore are denoted by M. The bands due to the *RS* complex are denoted by *.

2-Me-1-BuOH complex, together with the hole-burning spectra, are presented in Figure 2. As reported previously,⁶ chiral discrimination has been obtained in the fluorescence spectrum: the *SS* complex displays three main bands located at -134, -118 and -62 cm^{-1} from the origin of the bare molecule. The hole-burning experiments show that these features are due to two different isomers denoted hereafter IMSS1 and IMSS2, whose 0_0^0 transitions are located at -134 and -62 cm^{-1} , respectively. The IMSS1 complex shows a vibrational pattern built on a 16 cm^{-1} vibration. A similar vibration is observed for the IMSS2 isomer. The *RS* complex formation is revealed by the appearance of four main bands located at -84, -51, -34, and -19 cm^{-1} from the bare molecule origin. Hole-burning experiments have shown that three of them (-84, -51, -19 cm^{-1}) are due to the same isomer IMRS1 which exhibits a vibrational pattern built on a 33 cm^{-1} vibration. The feature located at -34 cm^{-1} does not appear clearly in the hole-burning spectra and cannot be assigned with certainty to the same isomer.

B. Secondary Alcohols. a. NapEtOH/2-Butanol (2-BuOH) Complexes. The fluorescence excitation spectrum of the NapEtOH/2-BuOH complex, together with the hole-burning spec-

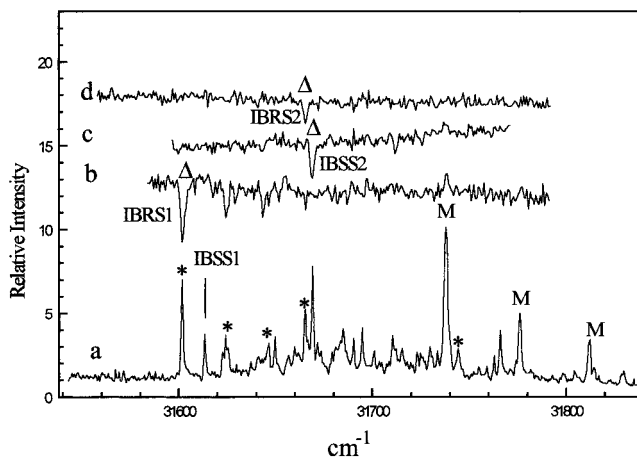


Figure 3. (a) Fluorescence excitation spectrum of the NapEtOH:2-butanol complex. Hole-burning spectrum obtained with the probe tuned on the transition located at (b) -136 cm^{-1} (RS complex), (c) -69 cm^{-1} (SS complex), (d) -73 cm^{-1} (RS complex). The probed band is denoted by Δ . The bands due to the bare chromophore are denoted by M. The bands due to the RS complex are denoted by *.

tra, are presented in Figure 3. The formation of the complex manifests itself by the appearance of five main bands in the fluorescence excitation spectrum. The excitation spectrum recorded with pure enantiomers has allowed assignment of the bands located at -136 , -114 , and -73 cm^{-1} from the origin of NapEtOH to the RS (SR) diastereoisomer and those located at -125 and -69 cm^{-1} from the origin to the SS (RR) complex.⁴ Hole-burning experiments show that four different isomers coexist in the jet, two of them correspond to the RS complex and the two others to the SS complex.

The 0_0^0 transitions of the RS isomers are located at -136 and -73 cm^{-1} from the 0_0^0 transition of the bare molecule: these isomers will be denoted IBRS1 and IBRS2 hereafter. The IBRS1 isomer shows (as IP1 in the case of the complex with 1-PrOH) a vibrational progression built on a 22 cm^{-1} vibration (bands at -114 cm^{-1} and -92 cm^{-1}). The 0_0^0 transition of the SS isomers are located at -125 and -69 cm^{-1} : these isomers will be denoted IBSS1 and IBSS2, respectively. Notice that IBRS2 and IBSS2 origins are only separated by 4 cm^{-1} (see Table 1) and that no vibrational feature appears for these isomers.

b. NapEtOH/2-Pentanol (2-POH) Complexes. Similar trends (the presence of several isomers for each diastereoisomer of the complex, with similar spectral shifts) have been observed for the NapEtOH/2-POH complex. The fluorescence excitation and hole-burning spectra of the NapEtOH/2-POH complex are shown in Figure 4. Depletion experiments clearly show that two isomers of the RS diastereoisomer are cooled in the jet: the first one, denoted hereafter IPRS1, shows a 0_0^0 band located at -147 cm^{-1} from the bare molecule origin, followed by a progression built on a 14 cm^{-1} mode. The second one displays a single weak band located at -52 cm^{-1} from the bare molecule origin. The depletion spectra of the SS diastereoisomer are more difficult to assign because of the superposition of bands: the hole-burning spectrum obtained with the probe fixed on the transition located at -54 cm^{-1} shows only this transition whereas the spectrum recorded with the probe fixed on the band at -84 cm^{-1} shows both bands at -84 and -54 cm^{-1} . This can be taken as an indication of the existence of two SS isomers: the first one is responsible for a single transition at -54 cm^{-1} ; the 0_0^0 band of the second one, located at -84 cm^{-1} , is followed by a 30 cm^{-1} vibration which is superimposed with the 0_0^0 band of the former.

TABLE 1: Assignment of the 0_0^0 Band and Main Transitions of the Different Ground-State Isomers of the NapEtOH:Propanol, NapEtOH:2-Butanol, NapEtOH:2-Propanol, NapEtOH:2-Methyl-1-butanol

complexing alcohol	isomer	shift (cm^{-1})
1-propanol	IP1	-138
	IP2	-112
	IP3	-60
	IMSS1	-55
2-methyl-1-butanol	IMSS1	-134
	IMRS1	-118
	IMSS2	-84
	IMRS2	-51
2-butanol	IBRS1	-62
	IBRS2	-34
	IBSS1	-136
	IBSS2	-114
2-pentanol	IPRS1	-125
	IPRS2	-73
	IPSS1	-69
	IPSS2	-147
		-133
		-119
		-85
		-52
		-54

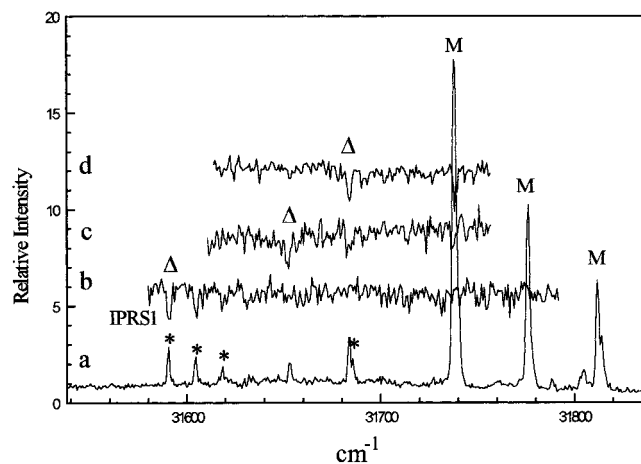


Figure 4. (a) Fluorescence excitation spectrum of the NapEtOH:2-pentanol complex. Hole-burning spectrum obtained with the probe tuned on the transition located at (b) -147 cm^{-1} (RS complex), (c) -84 cm^{-1} (SS complex), (d) -54 cm^{-1} (SS complex). The probed band is denoted by Δ . The bands due to the bare chromophore are denoted by M. The bands due to the RS complex are denoted by *.

We can draw the following conclusions from the experimental results:

(i) There are strong similarities between the spectral characteristics of the NapEtOH/1-PrOH and NapEtOH/2-BuOH complexes. A doublet is observed in the same energy range for both complexes and corresponds to two different isomers in the case of 1-PrOH (IP2, IP3) and two diastereoisomers in the case of 2-BuOH (IBRS2, IBSS2). The spectral separation in these doublets is around 5 cm^{-1} . Moreover, a similar progression (26 and 22 cm^{-1} , respectively) appears in the same energy range for IP1 and IBRS1. These similarities suggest a resemblance in geometries and interaction energies. Because of these spectroscopic similarities and because 1-propanol can be considered as a nonchiral model for 2-butanol (2-butanol is obtained by adding a methyl group in the 1 position of propanol), these systems have been chosen for detailed calculations.

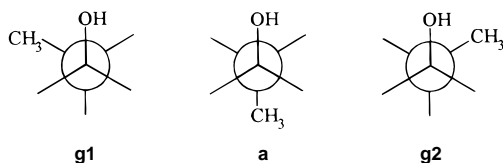
(ii) In the case of secondary alcohols, the RS complex gives rise to a larger red shift than the SS complex, while the reverse

situation holds for the complex with 2-Me-1-BuOH (primary alcohol). However, the excitation spectrum of the homochiral IMSS complex of 2-Me-1-BuOH is comparable (shift and vibrational structure) with the heterochiral IBRS complexes of 2-BuOH or IP1 of 1-PrOH. As the inversion in the shift of the electronic transition may reflect either an inversion in the relative interaction energy of *RS* and *SS* diastereoisomers in the ground state or in the excited state, we have also calculated the NapEtOH/2-Me-1-BuOH system.

2. Theoretical Model. A. Bare Molecules. a. Chromophore. First, the geometry of the chromophore has been optimized: as expected from experimental results, a single isomer is found. Several starting points have been used in the calculation, each of them leading to the same optimized geometry in which the O atom lies in the naphthalene plane and the hydroxyl H atom is out of the plane. This geometry is different from that of benzyl alcohol³⁴ for which an out of plane configuration of the OH group has been proposed. This difference probably results from the stronger steric hindrance introduced by the CH₃ substituent on the side-chain carbon.

Because of the mirror image relationship between the *RS* and *SR* (*RR* and *SS*) complexes, the calculations have been performed only with the *S* enantiomer of NapEtOH.

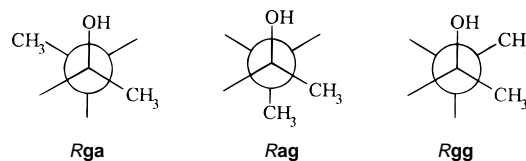
b. Solvents. 1-PrOH. Two gauche and one anti conformers of 1-PrOH have been calculated and are denoted **g1**, **g2**, and **a** respectively. The gauche conformer is more stable by 0.4 kcal/



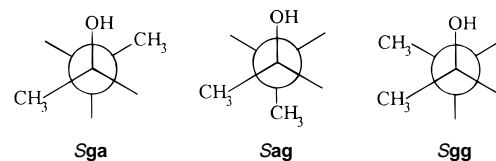
mol than the anti one. This is in agreement with the microwave spectrum of 1-PrOH which shows an energy difference of (0.29 ± 0.15) kcal/mol.²⁸ The attraction between the hydroxyl and methyl group is responsible for this difference in stability.²⁷ Studies of the cooling process in a supersonic expansion seeded with inert gases²⁶ indicate that under the conditions used here the relaxation of conformers is complete if the barrier for isomerization is low enough (less than 500 cm^{-1} [1.4 kcal/mol]). The barrier between two conformations is expected to be of the same order of magnitude as the barrier for rotation in ethane and in propane (≈ 3 kcal/mol),²⁷ so one can consider that the ground-state conformers do not interconvert in the supersonic expansion. It is important to notice here that under supersonic jet conditions the rotation around the C₁-C₂ axis is blocked and **g1** and **g2** must be considered as distinct conformers of 1-PrOH. As there is a mirror image relationship between them, **g1** and **g2** are axial enantiomers. So, at the low temperatures achieved in the jet, an axial chirality may be revealed by complexation with a chiral partner for molecules which are not chiral at room temperature. According to a Boltzmann distribution at room temperature, the relative populations are 40% of each gauche conformer and 20% of anti one. The calculations have been performed for the complexes of NapEtOH with the three possible conformers of 1-PrOH.

2-BuOH. The difference between 1-PrOH and the chiral secondary alcohol 2-BuOH is the substitution in the 1-position of a hydrogen atom by a methyl group. *R*-2-BuOH has three possible conformers, denoted hereafter as **Rga**, **Rag**, and **Rgg**. In this notation, the first index denotes the anti or gauche position of the OH relative to a CH₃ group, whereas the second

index denotes the relative position of both CH₃ groups. Thus the **ag** and **ga** conformations of the solvent are similar to *anti*- and *trans*-propanol respectively, following this scheme:

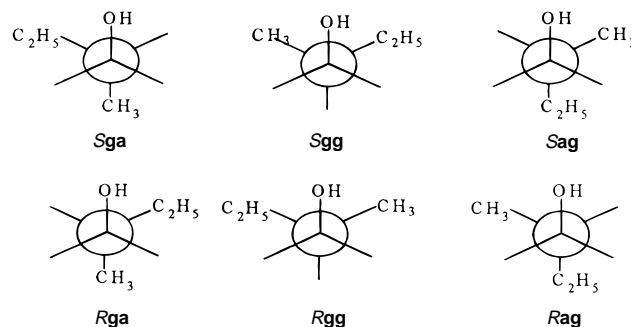


If now, we consider *S*-2-BuOH, there are also three conformers denoted hereafter, **Sga**, **Sag**, and **Sgg**, correspond to the following patterns:



The MP2-optimization of the geometry of these different conformers shows that the **ga** conformations are more stable than the **ag** and **gg** conformations and gives a difference of 0.8 kcal/mol between the energy of **ga** and **ag** and 1.2 kcal/mol between **ga** and **gg**. According to a Boltzmann distribution at room temperature, the relative populations of **ga**, **ag**, and **gg** are 0.72, 0.19, and 0.09, respectively. We have thus restricted the calculations to the most abundant conformers of 2-BuOH (**ga** and **ag**). We shall notice here that the **Rga** and **Sga** conformers of 2-BuOH are built from the **g1** and **g2** conformers of 1-PrOH, respectively, whereas the **Sag** or **Rag** forms of 2-BuOH correspond to the **a** conformer of 1-PrOH.

2-Met-1-BuOH. The MP2 optimization of the geometry of 2-Met-1-BuOH leads to six conformers whose energy differs by less than 0.1 kcal/mol. Thus, all the conformations of the solvent will be equally populated under supersonic jet conditions.



B. Complexes. In all the calculated complexes, the main interaction is a hydrogen bond between the alcohol groups of the solvent and the chromophore, where the NapEtOH acts as the hydrogen donor. The length of the H-bond is ~ 2.2 Å. This result is in good agreement with the observed red shift which has been explained by a H-bond from the OH group of the chromophore toward that of the solvent.⁶ Complexes where NapEtOH acts as an hydrogen bond acceptor have been found at higher energy and thus have not been taken into account. The results of interaction energies are summarized in Tables 2 and 3. The barriers for isomerization between complexes involving the same solvent conformer have been calculated and are summarized in Table 4. Either all of them are lower than 1.4 kcal/mol and/or one of the isomers is by far more stable

TABLE 2: Binding Energy of the Complexes of S-Naphthylethanol and the g1, g2, and a Conformations of Propanol, Together with Their Decomposition in Electrostatic, Dispersion, Polarization, and Repulsion Terms

propanol	E_{total}	$E_{\text{electrostatic}}$	$E_{\text{dispersion}}$	$E_{\text{polarization}}$	$E_{\text{repulsion}}$
Sg1	-6.533	-4.371	-5.534	-0.725	4.097
Sg1	-6.484	-5.035	-5.409	-0.764	4.725
Sg2	-6.537	-5.043	-5.256	-0.838	4.600
Sg2	-6.524	-4.902	-5.122	-0.743	4.243
Sa	-6.914	-4.602	-6.067	-0.699	4.454

TABLE 3: Binding Energy of the Complexes of S-Naphthylethanol and the Rga, Rag, Sga, and Sag Conformations of 2-Butanol, Together with Their Decomposition in Electrostatic, Dispersion, Polarization, and Repulsion Terms

2-butanol	E_{total}	$E_{\text{electrostatic}}$	$E_{\text{dispersion}}$	$E_{\text{polarization}}$	$E_{\text{repulsion}}$
RSga	-6.804	-4.699	-5.717	-0.733	4.346
RSga	-6.658	-4.377	-5.686	-0.734	4.141
RSga	-6.597	-4.883	-5.715	-0.739	4.740
RSag	-7.076	-4.596	-6.282	-0.706	4.508
SSga	-6.732	-4.833	-5.504	-0.744	4.352
SSga	-6.692	-5.002	-5.444	-0.834	4.588
SSga	-6.623	-5.184	-5.299	-0.767	4.628
SSag	-7.047	-4.773	-6.044	-0.754	4.524

TABLE 4: Calculated Barriers for Isomerizations between the Calculated Geometries of the Complexes between S-Naphthylethanol and g1 Propanol, g2 Propanol, Rga Butanol, Sga Butanol

complex	E_{total}^1	E_{total}^2	barrier
Sg1 propanol	-6.533	-6.484	0.922
Sg2 propanol	-6.537	-6.524	0.219
RSga butanol	-6.804	-6.658	0.971
RSga butanol	-6.658	-6.597	0.897
SSga butanol	-6.732	-6.692	0.152
SSga butanol	-6.692	-6.623	1.331

than the others: we may thus consider that a single isomer is formed in the jet for each enantiomer of a given conformation of the solvent.

a. NapEtOH/1-PrOH Complexes. Two stable isomers of the complexes with **g1** have been calculated with almost the same total interaction energy (-6.53 and -6.48 kcal/mol). The only difference is the respective contribution to the total energy of the electrostatic and repulsion terms which almost cancel each other. For the first isomer the result of the decomposition gives $E_{\text{electrostatic}} = -4.37$ kcal/mol and $E_{\text{repulsion}} = 4.10$ kcal/mol whereas for the second one the corresponding values are -5.03 and 4.72 kcal/mol respectively. The dispersion and polarization terms are the same for both isomers. In the case of the **g2** conformer, again two stable isomers have been obtained with almost the same total interaction energy (-6.54 and -6.52 kcal/mol). All the isomers, formed with the gauche conformers of 1-PrOH, exhibit an extended geometry: the alkyl chain lies out of the plane of the aromatic ring of the chromophore. This is illustrated in Figure 5a for the complex with **g2**.

The complex with the anti conformer leads to clearly different results: it exhibits by far a larger stabilization energy (-6.91 kcal/mol) than all those with the gauche conformers. This stabilization does not result from the electrostatic term (see Table 2) but from the dispersion component which is larger by at least 0.5 kcal/mol than any of the other calculated complexes. This complex exhibits a folded geometry: the alkyl chain is bent over the aromatic ring of the chromophore, which explains the higher dispersion energy term (see Figure 5b). A more detailed analysis of the interaction energy shows that the two H atoms in the 1-position of propanol have distinct properties: while

one of the H atoms does not bring an important contribution to the interaction energy, there is a strong repulsion between the other H atom and the aromatic ring.

b. NapEtOH/2-BuOH Complexes. The interaction energies of the calculated isomers, together with the partition between electrostatic, dispersion, repulsion, and polarization terms are summarized in Table 3.

As has been obtained in the case of the anti conformer of 1-PrOH, the complexes involving the **ag** conformers (identical for *R* and *S*-2-BuOH) are always stabilized more than those with all the other conformations (*RS*: -7.08 kcal/mol, *SS*: -7.05 kcal/mol). These complexes exhibit a folded geometry. For the *RS* diastereoisomer, the ethyl group lies above the aromatic ring whereas the methyl group is outside and does not show any interaction with the ring. The geometry of the *SS* complex is intermediate since neither the methyl nor the ethyl group stands above the aromatic ring but both alkyl groups are close in distance from it. Moreover, these isomers exhibit an important dispersion term (*RS*: -6.28 kcal/mol, *SS*: -6.04 kcal/mol) compared with those found with **ga** conformers. These complexes are shown in Figure 6.

For the *S*-NapEtOH/**ga** complexes, six isoenergetic isomers are calculated, similar to the complexes with the **g1** and **g2** conformers of 1-PrOH. The main differences between them consist in the balance between electrostatic and repulsion components of the total interaction energy: the dispersion term is equivalent for all the isomers. For *RS* complexes, the total interaction energies are -6.80, -6.66, and -6.60 kcal/mol, respectively, for each complex and the balance is $E_{\text{electrostatic}} = -4.70$ kcal/mol vs $E_{\text{repulsion}} = 4.35$ kcal/mol for the first complex (-4.38/4.14 and -4.88/4.74, respectively, for the others). For *SS* complexes, the total interaction energies are -6.73, -6.69, and -6.62 kcal/mol, respectively, for each complex and the balance is $E_{\text{electrostatic}} = -4.83$ kcal/mol vs $E_{\text{repulsion}} = 4.35$ kcal/mol for the first complex (-5.00/4.59 and -5.18/4.63, respectively, for the following ones). All these complexes exhibit an extended geometry. The characteristics of the *S*-NapEtOH/2-BuOH calculated complexes are thus very similar to that of the *S*-NapEtOH/1-PrOH complexes.

Finally, we can note that in a general way, more than 85% of the attractive interaction in the **ag** complexes is due to dispersion, which contrasts with the **ga** complexes.

c. NapEtOH/2-Met-1-BuOH Complexes. Calculations have also been performed for this system in order to explain the reverse order between the shift of the *SS* and *SR* diastereoisomers relative to secondary alcohols. Numerous conformations may be adopted by this solvent molecule, and calculations have been performed on the **gg**, **ag**, **ga** conformations of the solvent in order to observe general trends. Several general conclusions can be drawn:

(i) For each **gg**, **ag**, **ga** conformer of the solvent, the *SS* complex is always more stable than the *RS* complex.

(ii) Accordingly, for all the conformations of the solvent, the *SS* complex shows an important dispersion term (up to 7.3 kcal/mol). This is not true for the *RS* complex for which the dispersion term is always smaller than 6.7 kcal/mol.

(iii) The geometry of the *SS* and *RS* diastereoisomers differ by the position of the C_2H_5 chain of the alcohol molecule relative to the naphthalene ring. In the homochiral pair, the C_2H_5 chain is bent over the ring, whereas in the heterochiral pair, this position is occupied by the CH_3 group. These geometries are illustrated in Figure 7.

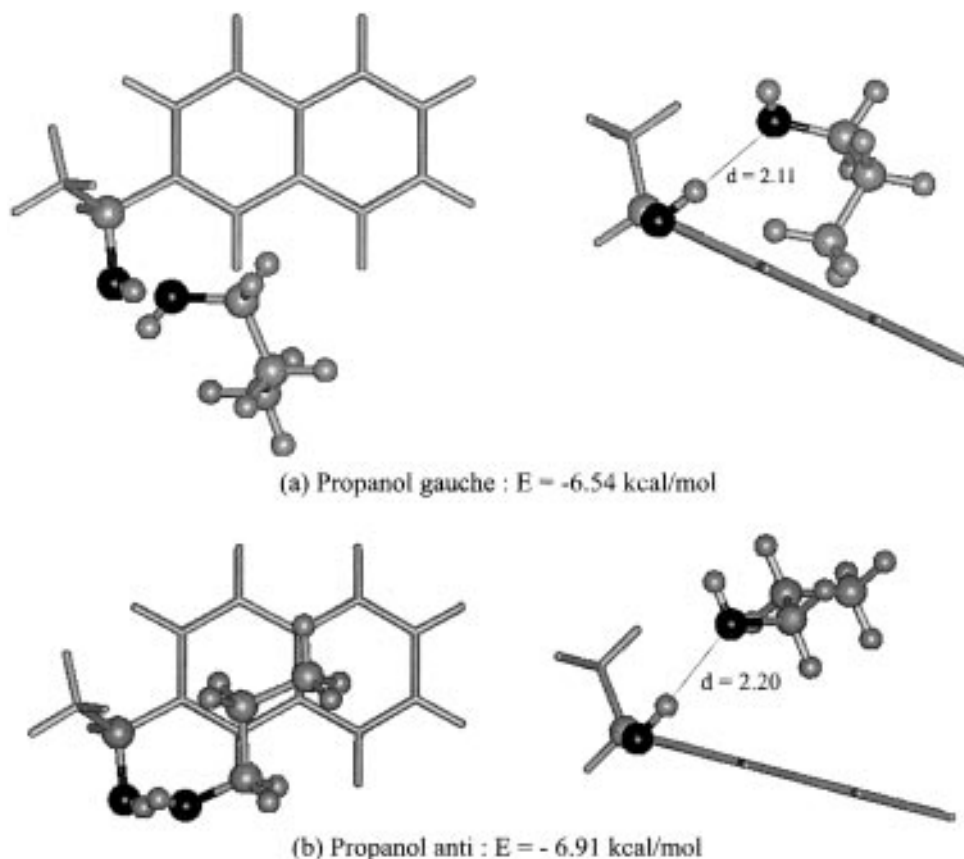


Figure 5. Calculated geometry of the NapEtOH complex with (a) *g2* propanol and (b) *a* propanol (note the repulsion between a hydrogen atom and the aromatic ring).

Discussion

We will now discuss a tentative assignment of the calculated complexes to the different isomers observed in the hole-burning experiments. It is based on the following hypotheses:

(i) the spectral characteristics between the complexes of NapEtOH with 1-PrOH and 2-BuOH (similar red shift and vibrational progression) must correspond to similarities between the calculated structures. Thus, the comparison between the two systems can be used to assess the proposed attribution.

(ii) Since the fluorescence lifetimes have been shown to depend strongly on the excited feature, which reveals an irregular change in the fluorescence quantum yield of the excited complexes, the intensity of the bands observed in the excitation spectrum cannot be taken as an indication of the ground-state populations.

(iii) The S_0-S_1 transition involving the π electrons of the naphthalene ring does not strongly modify the electronic distribution on the OH group of the chromophore. This hypothesis is reinforced by a very small difference in the transition energy of NapEtOH (31738 cm^{-1}) relative to 2-methylnaphthalene in the gas phase (31699 cm^{-1})³⁵. Moreover, the contribution of the electrostatic component to the total interaction energy does not change significantly for all the calculated complexes. Thus, the modification of the electrostatic part of the interaction energy upon excitation may not be the main discriminating factor for the spectroscopic behaviors of the isomeric complexes of NapEtOH with aliphatic alcohols. We shall thus consider that the dispersion forces are generally responsible for an increased stabilization of the excited-state relative to the ground state of the complex: the higher the dispersion in the ground state, the larger the red shift of the electronic transition.

1. Comparison between with 1-PrOH and 2-BuOH. *a. The Most Red-Shifted Isomers: IP1 Compared with IBRS1 and IBSS1.* Under the reasonable assumption that the complex which exhibits the most important dispersion term corresponds to the most red-shifted isomer (hypothesis iii), we may associate the IP1 isomer of 1-PrOH complex (located at -138 cm^{-1} from the origin) with the complex involving the anti conformer of 1-PrOH. This hypothesis is reinforced by the fluorescence excitation spectra of complexes of NapEtOH with short chain alcohols such as methanol or ethanol.⁶ These additional spectra do not display any feature in the range of -130 to -140 cm^{-1} from the bare molecule origin and exhibit mainly an intense single band at around -70 cm^{-1} which is also present in the excitation spectrum of all the complexes. This shift may thus correspond to the shift of the electronic transition induced by the H-bond, without the participation of the dispersive interactions due to the folding of the alkyl chain onto the aromatic ring. This can be understood since the short size of the alkyl chain of the alcohol molecule prevents any folded conformation (without breaking the H-bond which is the main interaction) and thus reduces the dispersion term and the red shift. This attribution is also compatible with the observation of a low-frequency (around 15 cm^{-1}) mode. The activity of this mode is related to a difference in the equilibrium geometry in the ground and the excited states. As the excitation is mainly localized on the π system, this must be due to a modification upon excitation of the dispersive forces between the aromatic ring and the alkyl chain of 1-PrOH. Wagging or slipping motions of the alkyl chain relative to the aromatic ring may be good candidates for this mode, which is obviously not active in the extended geometry of the complex.

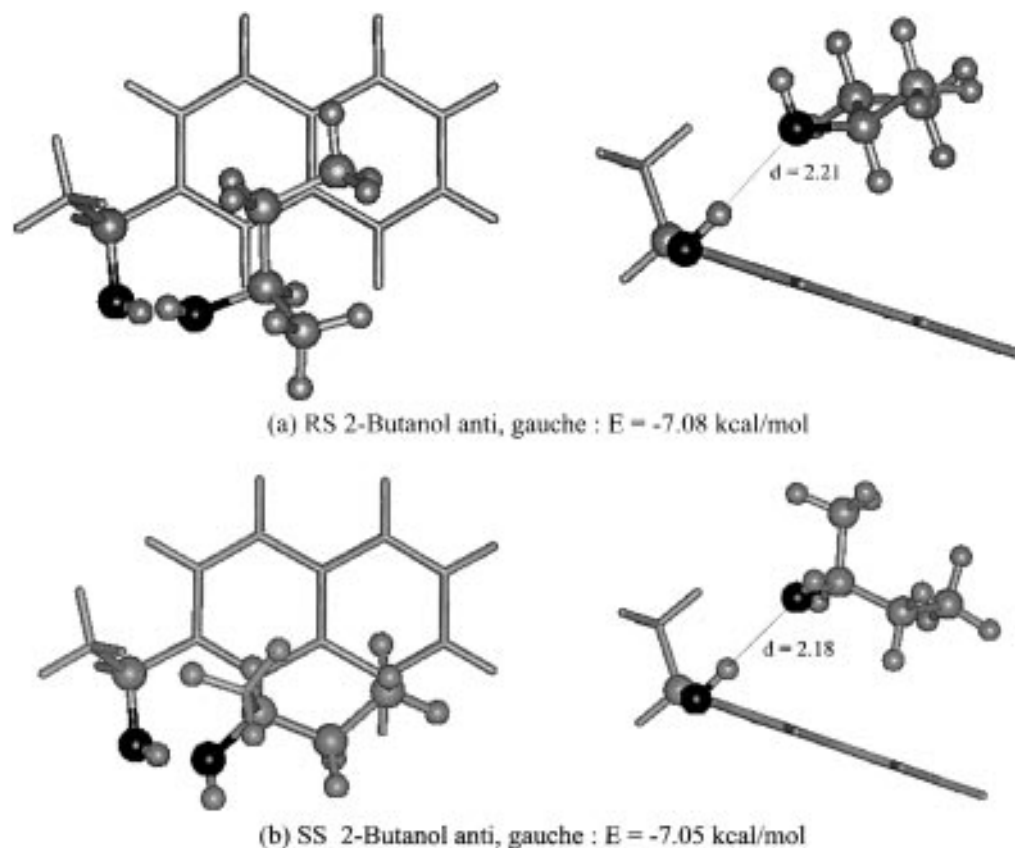


Figure 6. Calculated geometry of the NapEtOH: **ag** 2-butanol complex. a) *RS* diastereoisomer. Note that this conformation is very similar to that of the NapEtOH: **a** 1-propanol complex. b) *RR* diastereoisomer. Note that steric hindrance induces a strong distortion of this complex relative to the NapEtOH: **a** 1-propanol complex.

We may apply the same consideration to the *R*-2-BuOH/*S*-NapEtOH complexes and assign the most stable *RSag* calculated complex to the most red-shifted isomer (IBRS1) observed in the hole-burning experiment. The *RSag* (for *R*-2-BuOH) and *Sa* (for 1-PropOH) complexes have very similar geometries, which explains the similarity between their spectroscopic properties (see Figures 5b and 6a). The ethyl chain is in the same position in both complexes and interacts strongly with the ring. In the case of *R*-2-BuOH, the H atom of the chiral center is in the same position as the H atom of propanol, which shows a repulsive interaction with the ring, and the added methyl group is away from the naphthalene ring, its presence modifies neither the complex geometry nor its interaction energy. In particular, the repulsion does not increase when changing from 1-PrOH to *R*-2-BuOH.

The most red-shifted *SS* diastereoisomer (IBSS1) can also be assigned to the most stable *SSag* calculated complex. However, we observe in Figure 6b that the geometry of this complex cannot be simply deduced from that of the *Sa* isomer of the 1-PrOH/NapEtOH complex. The position of the CH₃ group and the H atom of the chiral center are inverted in *Sag* 2-BuOH relative to the *Rag* enantiomer. An increased repulsion is thus introduced when H is replaced by CH₃, which leads to a switch of the ethyl group on the edge of the ring and in a decrease in dispersive interactions. This distorted geometry may explain the smaller red shift and the absence of any vibrational pattern in the *Sag*/NapEtOH relative to the *Rag* complex.

This example clearly shows that, in this case, the chiral discrimination is achieved by means of the repulsion–dispersion part of the interaction energy.

b. The Less Red-Shifted Doublet: IP2, IP3 Compared with IBRS2, IBSS2. As mentioned previously, the excitation spec-

trum of both complexes with 1-PrOH and 2-BuOH exhibits a slightly red-shifted ($\approx -60 \text{ cm}^{-1}$) doublet with a small separation ($\approx 5 \text{ cm}^{-1}$) which has been shown to arise from different isomers. In the case of 2-BuOH, these isomers are different diastereoisomers. As discussed previously, the *Rga* and *Sga* enantiomers of 2-BuOH are built from the **g1** and **g2** conformers of 1-PrOH. Moreover, there is a strong resemblance between the calculated structures of the **g1** and the *Rga* complexes, and the **g2** and the *Sga* complexes, respectively. Because of these correlations between the spectral characteristics and the calculated structures, the IP2 and IP1 isomers of 1-propanol corresponding to the doublet are assigned to the complexes with **g1** and **g2**. Several conformations have been calculated with close interaction energy for the **g1** and **g2** complexes. For all of them, there is no folding of the alkyl chain on the naphthalene ring, which explains the small spectral differentiation. It has to be stressed here that despite the fact that the alkyl chain lies away from the naphthalene ring, which means that the ring “does not see” if the solvent is in the **g1** or **g2** conformation, a spectral discrimination, even though weak (5 cm^{-1}), is observed.

It is however not possible to decide which of the calculated isomers of the *R*-2-BuOH (respectively *S*-2-BuOH) corresponds to the experimental data. There is a close resemblance between the calculated complexes with **g1** (respectively **g2**) conformers of 1-PrOH and the *RSga* and *SSga* complexes. Thus, in the doublet, IP2 (IP3 respectively) may be assigned to a complex with the *Sg1* (*Sg2* respectively) conformer of 1-PrOH, and IBRS2 (IBSS2 respectively) isomers of the complex with 2-BuOH may be assigned to the *RSga* (*SSga* respectively) conformer. It is interesting to stress here that the chiral discrimination obtained with the stable optical isomers of 2-BuOH

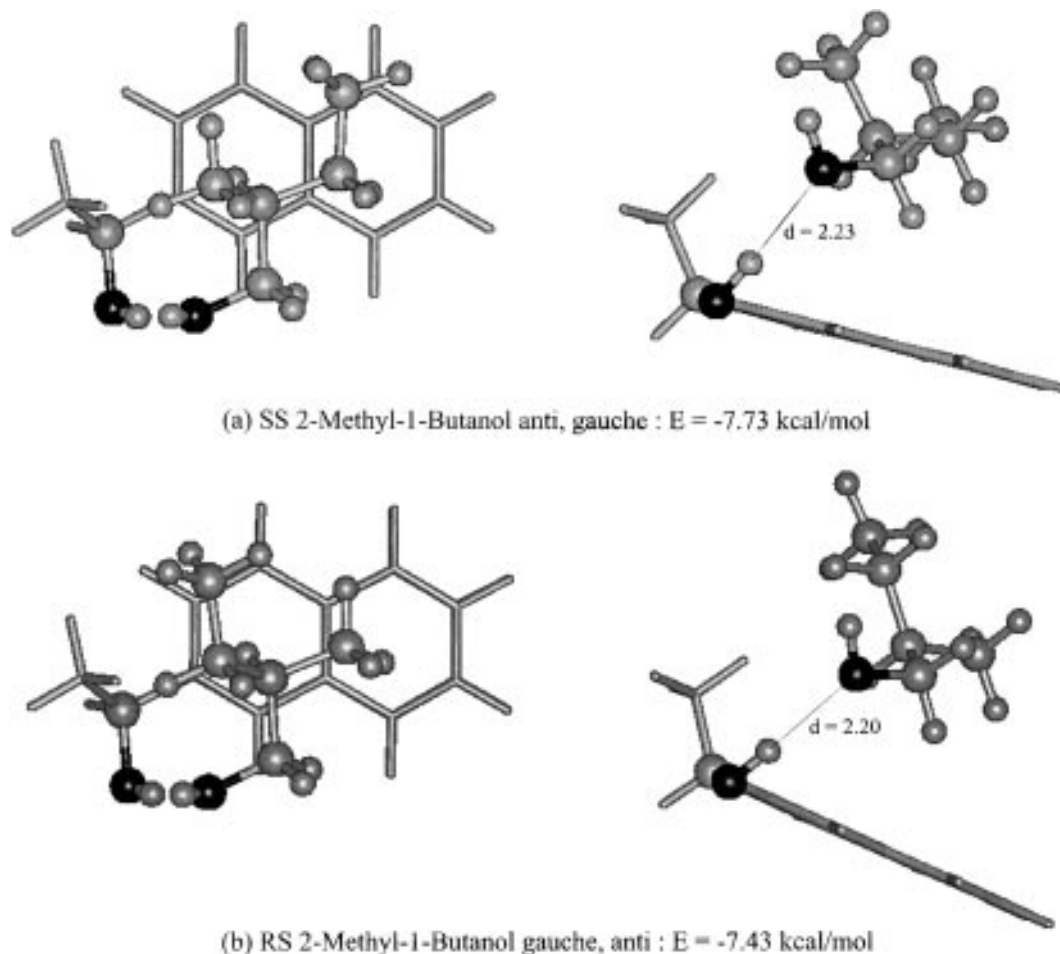


Figure 7. Calculated geometry of the NapEtOH: 2-methyl-1-butanol complex: (a) *SSag* complex, (b) *RSga* complex. Note the position of the C_2H_5 group of 2-methyl-1-butanol relative to the naphthalene ring, which leads to a strong dispersive interaction in the case of the *SS* complex.

enlightens the spectral behavior of the complexes involving 1-PrOH by providing an explanation of the origin of the IP1 and IP2 discrimination as being due to the presence of rotational enantiomers of 1-PrOH which cannot be separated at room temperature.

2. 2-Me-1-BuOH. The main experimental observation is that the *SS* complex shows the largest red shift together with a long progression. As the calculations show that there are two *SS* diastereoisomers with a large dispersion component (**ga** and **ag**), it is tempting to assign the observed progression to one of these *SS* complexes. The specificity of 2-Me-1-BuOH is that in this system, no *RS* pair involves a large dispersion component: this leads to a high discrimination between both diastereoisomers. Figure 7 illustrates this property with the example of the *RSga* and *SSag*: one can see clearly that in the case of the *SS* complex, the ethyl group interacts strongly with the aromatic ring, which leads to a large dispersion term. This is clearly not the case for the *RS* complex. The same behavior is qualitatively observed for the other conformations of the solvent, where the bulky CH_3 group interacts with the naphthalene subunit.

It has to be stressed finally that, at least for the specific complexes presented here, the most stable complex is always the most red-shifted in the excitation spectrum.

Conclusion

Depletion spectroscopy experiments combined with theoretical calculations on van der Waals complexes between a chiral naphthalene molecule and aliphatic alcohol have demonstrated

the formation of isomers that involve different conformations of the solvent. This investigation has allowed a rationalization of the spectroscopic enantiodiscrimination mechanism observed in these simple systems by using 1-propanol as the ligand model. All the complexes are bound by a H-bond which provides the main localized electrostatic interaction site between the two partners. The discrimination between the *RR* and *RS* complexes with chiral alcohols has been shown to depend on the solvent conformation: the largest discrimination is observed for the anti conformation of the solvent. This effect has been related to a difference in the dispersive forces which are more important for the anti conformer. It is thus important for the understanding of the enantioselectivity to consider the conformational control exerted in van der Waals interactions between flexible chiral molecules. In the systems under study, the less stable anti conformation of the solvent, which is less populated at room temperature, exhibits the larger chiral discrimination. The dispersive forces involved in this case are due to the intermolecular forces between the aromatic ring of the chromophore and the alkyl chain of the solvent, which leads to a folded geometry and provides a further site of selective interaction. Thus, provided that the chiral solvent adopts a conformation that allows an interaction with the aromatic ring (through the dispersion–repulsion part of the interaction energy), chiral discrimination will be obtained. Further investigation using bifunctional molecules (dialcohol or amino alcohol) is in progress: a second localized interaction by means of a H-bond between one of the functional hydrogen atoms and the π system of the aromatic ring is expected to bring a more rigid and

specific structure of the complexes, improving the enantioselectivity. A second concluding observation is that a precise examination of the partition of the interaction energy shows that a difference in the total ground-state interaction energy is not necessary to differentiate between diastereoisomers, provided that the different terms of the interaction energy differ for both diastereoisomers. As the different terms do not vary in the same way upon excitation, a different shift of the excitation spectrum is expected: this can be seen, for example, with 2-butanol for which the total energy is the same for the *SSag* and *RSag* forms but not the relative amount of dispersion and electrostatic interaction. This last consideration shows the sensitivity of the method described here.

References and Notes

- (1) Cantor, L. R.; Schimmel P. R. *Biophysical Chemistry*; Freeman: San Francisco, 1980.
- (2) Parker, D. *Chem. Rev. (Washington, D.C.)* **1991**, *91*, 1441.
- (3) Pirkle, W. H.; Pochapsky T. G. *Chem. Rev. (Washington, D.C.)* **1989**, *89*, 347.
- (4) Rau, H. *Chem. Rev. (Washington, D.C.)* **1983**, *83*, 535.
- (5) Al-Rabaa, A. R.; Br  h  ret, E.; Lahmani, F.; Zehnacker, A. *Chem. Phys. Lett.* **1995**, *237*, 480.
- (6) Al-Rabaa, A. R.; Le Barbu, K.; Lahmani, F.; Zehnacker-Rentien, A. *J. Phys. Chem.* **1997**, *101*, 3273.
- (7) Al-Rabaa, A. R.; Le Barbu, K.; Lahmani, F.; Zehnacker-Rentien, A. *J. Photochem. Photobiol. A Chem.* **1997**, *105*, 277.
- (8) Lipert, R. J.; Colson, S. D. *Chem. Phys. Lett.* **1989**, *161*, 303.
- (9) Lahmani, F.; Sepiol, J. *Chem. Phys. Lett.* **1992**, *189*, 479.
- (10) Piuzzi, F. *Chem. Phys. Lett.* **1993**, *209*, 484.
- (11) Topp, M. R. *Int. Rev. Phys. Chem.* **1993**, *12*, 149 and references therein.
- (12) Zehnacker, A.; Lahmani, F.; Piuzzi, F. *Trends Phys. Chem.* **1994**, *4*, 243 and references therein.
- (13) Sun, S.; Bernstein, E. R. *J. Am. Chem. Soc.* **1996**, *118*, 5086.
- (14) Brenner, V.; Zehnacker-Rentien, A.; Lahmani, F.; Milli  , P. *J. Phys. Chem.* **1993**, *97*, 10570 and references therein.
- (15) Iwanek, W.; Mattay, J. *J. Photochem. Photobiol. A Chem.* **1992**, *67*, 209.
- (16) Hanessian, J.; Simard, M.; Roelens, S. *J. Am. Chem. Soc.* **1995**, *117*, 7630.
- (17) Dagleish, C. E. *J. Chem. Soc.* **1952**, 3940.
- (18) Lahmani, F.; Zehnacker-Rentien, A. *Chem. Phys. Lett.* **1997**, *271*, 6.
- (19) Claverie, P. In *Intermolecular Interactions from diatomics to biopolymers*; Pullman, B., Ed.; Wiley: New York, 1978.
- (20) Tramer, A.; Piuzzi, F.; Brenner, V. *J. Photochem. Photobiol. A Chem.* **1994**, *80*, 95.
- (21) Brenner, V.; Martrenchard-Barra, S.; Milli  , P.; Dedonder-Lardeux, C.; Jouvet, C.; Solgadi, D. *J. Phys. Chem.* **1995**, *99*, 5848.
- (22) Brenner, V.; Milli  , P. *Z. Phys. D* **1994**, *30*, 327.
- (23) Hehre, W. J.; Stewart, R. F.; Pople, J. A. *J. Chem. Soc.* **1969**, *51*, 2657.
- (24) Dewar, M. J. S.; Zoebisch, E. G.; Healy, E. F.; Stewart, J. P. P. *J. Am. Chem. Soc.* **1985**, *107*, 3902. Frisch, M. J.; Trucks, G. W.; Schlegel, H. B.; Gill, P. M. W.; Johnson, B. G.; Robb, M. A.; Cheeseman, J. R.; Keith, T.; Petersson, G. A.; Montgomery, J. A.; Raghavachari, K.; Al-Laham, M. A.; Zakrzewski, V. G.; Ortiz, J. V.; Foresman, J. B.; Cioslowski, J.; Stefanov, B. B.; Nanayakkara, A.; Challacombe, M.; Peng, C. Y.; Ayala, P. Y.; Chen, W.; Wong, M. W.; Andres, J. L.; Replogle, R. S.; Gomperts, R.; Martin, R. L.; Fox, D. J.; Binkley, J. S.; Defrees, D. J.; Baker, J.; Stewart, J. P.; Head-Gordon, M.; Gonzalez, C.; Pople, J. A. *Gaussian 94, Revision C.2*; Gaussian, Inc.: Pittsburgh, PA, 1995.
- (25) Ruoff, R. S.; Klots, D. E.; Emilsson, T.; Gutowsky, H. S. *J. Chem. Phys.* **1990**, *93*, 3142.
- (26) Eliel, E. L.; Wilen, S. H. *Stereochemistry of organic compounds*; Wiley: New York.
- (27) Kagan, H. *La st  r  ochimie organique*; Presses Universitaires de France: Paris, 1975.
- (28) Vigne-Mader, F.; Claverie, P. *J. Phys. Chem.* **1988**, *88*, 4934.
- (29) Bockish, F.; Liotard, D.; Rayez, J. C.; Duguay, B. *Int. J. Quantum Chem.* **1992**, *44*, 619.
- (30) (a) Kirkpatrick, P. *J. Stat. Phys.* **1984**, *34*, 975. (b) Press, W. H.; Flannery, B. P.; Teukolsky, S. A.; Wetterling, W. T. *Numerical recipes, the art of scientific computing*; University Press: Cambridge, 1986; Chapter 10.
- (31) Liotard, D. *Int. J. Quantum Chem.* **1992**, *44*, 723.
- (32) Ichimura, T.; Auty, A. R.; Jones, A. C.; Phillips, D. *J. Chem. Soc. Jpn.* **1985**, *58*, 2407.
- (33) Im, H. S.; Bernstein, E. R.; Secor, H. V.; Seeman, J. I. *J. Am. Chem. Soc.* **1993**, *113*, 4422. Warren, J. M.; Haynes, J. M.; Small, G. J. *J. Chem. Phys.* **1986**, *102*, 313.